SINTEF
PROCEEDINGS
2

Proceedings of the 12th International Conference on Computational Fluid Dynamics in the Oil & Gas, Metallurgical and Process Industries

Progress in Applied CFD – CFD2017

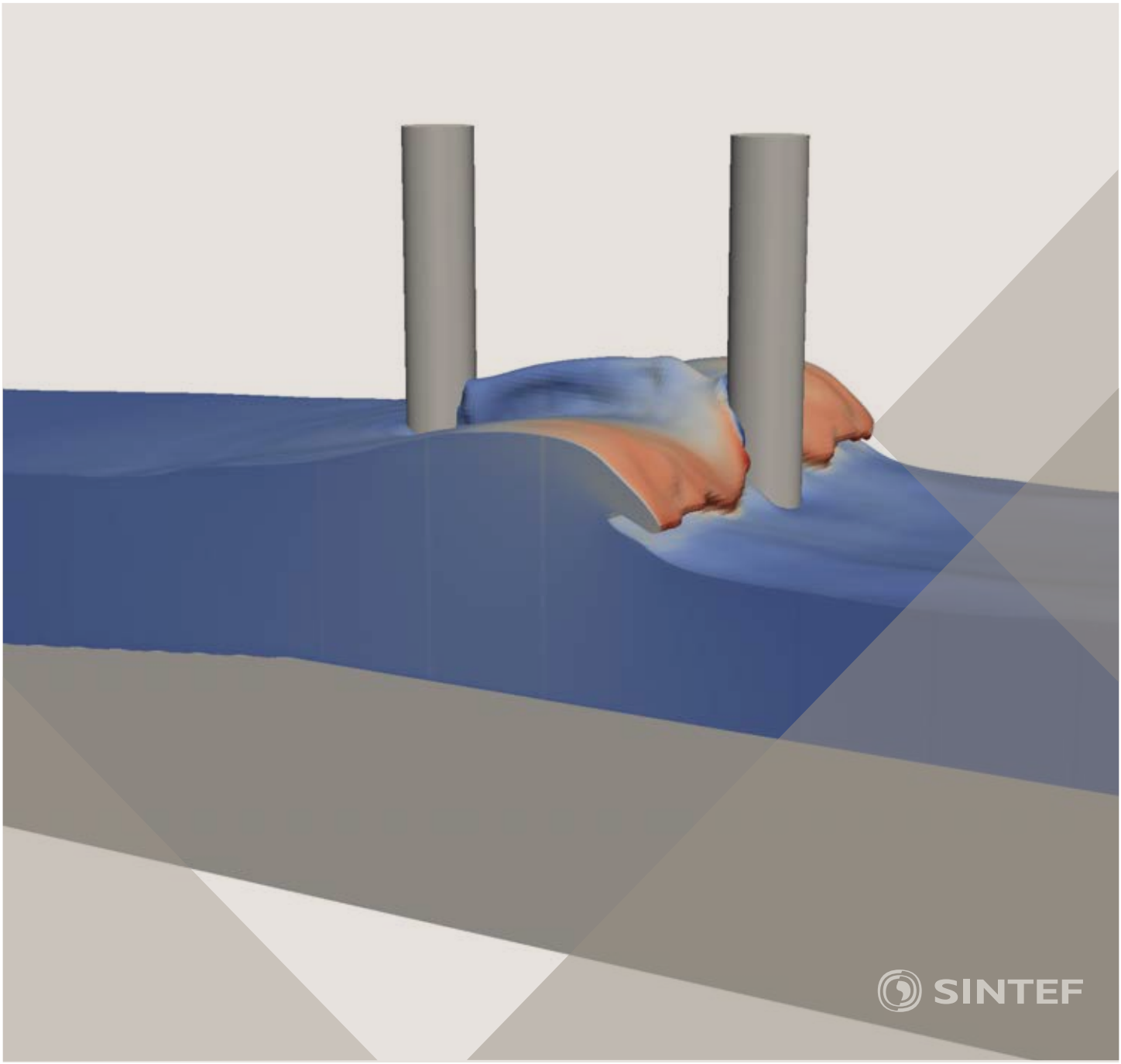

SINTEF Proceedings

Editors:
Jan Erik Olsen and Stein Tore Johansen

Progress in Applied CFD – CFD2017

Proceedings of the 12th International Conference on Computational Fluid Dynamics in the Oil & Gas, Metallurgical and Process Industries

SINTEF Academic Press

SINTEF Proceedings no 2
Editors: Jan Erik Olsen and Stein Tore Johansen
Progress in Applied CFD – CFD2017
Selected papers from 10th International Conference on Computational Fluid Dynamics in the Oil & Gas, Metallurgical and Process Industries

Key words:
CFD, Flow, Modelling

Cover, illustration: Arun Kamath

ISSN 2387-4295 (online)
ISBN 978-82-536-1544-8 (pdf)

SINTEF Academic Press
Address: Forskningsveien 3 B
PO Box 124 Blindern
N-0314 OSLO
Tel: +47 73 59 30 00
Fax: +47 22 96 55 08

www.sintef.no/byggforsk
www.sintefbok.no

SINTEF Proceedings
SINTEF Proceedings is a serial publication for peer-reviewed conference proceedings on a variety of scientific topics.
The processes of peer-reviewing of papers published in SINTEF Proceedings are administered by the conference organizers and proceedings editors. Detailed procedures will vary according to custom and practice in each scientific community.

PREFACE

This book contains all manuscripts approved by the reviewers and the organizing committee of the 12th International Conference on Computational Fluid Dynamics in the Oil & Gas, Metallurgical and Process Industries. The conference was hosted by SINTEF in Trondheim in May/June 2017 and is also known as CFD2017 for short. The conference series was initiated by CSIRO and Phil Schwarz in 1997. So far the conference has been alternating between CSIRO in Melbourne and SINTEF in Trondheim. The conferences focuses on the application of CFD in the oil and gas industries, metal production, mineral processing, power generation, chemicals and other process industries. In addition pragmatic modelling concepts and bio-mechanical applications have become an important part of the conference. The papers in this book demonstrate the current progress in applied CFD.

The conference papers undergo a review process involving two experts. Only papers accepted by the reviewers are included in the proceedings. 108 contributions were presented at the conference together with six keynote presentations. A majority of these contributions are presented by their manuscript in this collection (a few were granted to present without an accompanying manuscript).

The organizing committee would like to thank everyone who has helped with review of manuscripts, all those who helped to promote the conference and all authors who have submitted scientific contributions. We are also grateful for the support from the conference sponsors: ANSYS, SFI Metal Production and NanoSim.

Stein Tore Johansen & Jan Erik Olsen

Organizing committee:

Conference chairman: Prof. Stein Tore Johansen
Conference coordinator: Dr. Jan Erik Olsen
Dr. Bernhard Müller
Dr.Sigrid Karstad Dahl
Dr.Shahriar Amini
Dr.Ernst Meese
Dr.Josip Zoric
Dr.Jannike Solsvik
Dr.Peter Witt

Scientific committee:

Stein Tore Johansen, SINTEF/NTNU
Bernhard Müller, NTNU
Phil Schwarz, CSIRO
Akio Tomiyama, Kobe University
Hans Kuipers, Eindhoven University of Technology
Jinghai Li, Chinese Academy of Science
Markus Braun, Ansys
Simon Lo, CD-adapco
Patrick Segers, Universiteit Gent
Jiyuan Tu, RMIT
Jos Derksen, University of Aberdeen
Dmitry Eskin, Schlumberger-Doll Research
Pär Jönsson, KTH
Stefan Pirker, Johannes Kepler University
Josip Zoric, SINTEF

CONTENTS

AN EULER-EULER MODEL FOR GAS-LIQUID FLOWS IN A COIL WOUND HEAT EXCHANGER

Thomas ACHER[1]*, **Manuel KNAUP**[1], **Konrad BRAUN**[1], **Hans-Jörg ZANDER**[1]

[1]The Linde Group - Engineering Division, Dr.-Carl-von-Linde-Straße 6-14, 82049 Pullach, GERMANY

* E-mail: thomas.acher@linde.com

ABSTRACT

Coil-wound heat exchangers (CWHE) are commonly adapted in process engineering for the efficient transfer of heat between fluids which feature wide temperature and pressure ranges. The field of application for this apparatus ranges from heating or cooling of single-phase flows, over the evaporation or condensation of fluids, to the utilization as isothermal reactor. Due to their large specific heat transfer area accompanied by a compact design, coil-wound heat exchangers are widely used in various process plants (e.g., LNG plants). Depending on the application, two-phase flows may occur at both, the tube- as well as the shell-side of the apparatus. For the design of a CWHE, the fluid and thermodynamic processes in the unit are commonly represented by a system of one-dimensional correlations. This approach implies uniform thermohydraulic conditions on horizontal cutting planes of the exchanger. Fluid and thermodynamic effects in the apparatus which result in radial parameter variations are inaccessible to these conventional design tools. To this end, a multidimensional CFD model has been established to enhance the representation of fluid and thermodynamic phenomena in CWHE design. The shell-side of the CWHE and all tube-side sections are each numerically represented by separate domains which are coupled by source terms to account for the thermodynamic interaction between tube- and shell-side. In each flow region, the hydraulic effect of the tube bundle is modeled as a porous medium with corresponding fluid dynamic characteristics. The gas-liquid dynamics in each flow region is modeled based on an Euler-Euler approach. Unlike classical Euler-Euler models, local phase fractions and fluid properties are calculated from species relations as well as pressure and temperature fields. This model framework is augmented by locally evaluated correlations for pressure drop and heat transfer to account for apparatus internals and thermal coupling. The models for gas-liquid interaction forces are derived from standard correlations and augmented by findings from detailed CFD studies. Remaining parameters are specified by a parameterization study based on experimental findings.

Keywords: process industry, heat exchanger, multiphase heat transfer, Euler-Euler approach.

NOMENCLATURE

Greek Symbols

α	Phase volume fraction, $[-]$
ε	Porosity, $[-]$
ρ	Mass density, $[kg/m^3]$
$\underline{\tau}$	Stress tensor, $[N/m^3]$

Latin Symbols

a	Velocity profile coefficient, $[-]$.
A	Area, $[m^2]$.
C	Model constant, $[-]$.
$\vec{f}$	Volumetric force, $[kg/ms^2]$.
g	Gravitational acceleration, $[m/s^2]$.
p	Pressure, $[Pa]$.
$\vec{u}$	Velocity, $[m/s]$.

Sub/superscripts

ax	Axial.
$cent$	Centrifugal force.
g	Gas.
h	Homogeneous.
i	Phase indicator.
j	Phase indicator.
l	Liquid.
$lift$	Lift force.
rad	Radial i.

INTRODUCTION

In various process engineering applications coil-wound heat exchangers (CWHE) are adopted for the efficient transfer of heat between fluids. The potential operating conditions of this type of apparatus feature a wide range of temperature and pressure levels and the transfer of heat between multiple fluid streams can be realized in one heat exchanger. CWHEs are specifically robust to transients of flow properties (Pacio and Dorao, 2011) and are characterized by a large specific heat transfer area per volume in combination with a comparably compact design. In a CWHE, multiple layers of tubes are wound helically around a central pipe (see Fig. 1) where several tubes are grouped into sections with varying fluid streams. Apparatuses with up to 10,000 tubes enable complex heat exchange processes with heating surfaces of 30,000 m^2 and more. Maximal bundle diameters of approx. 5,500 mm and unit heights up to 20 meters can be manufactured. (Walter *et al.*, 2014)

In many large scale plants for the production of liquified natural gas (LNG) CWHEs represent a key equipment. In these applications, the gaseous natural gas is fed to tube sections at the bottom of the apparatus and is cooled, liquefied or subcooled while streaming upwards. In the

remaining tube sections the refrigerant is precooled by streaming concurrent to the natural gas. Subsequently, the refrigerant is applied to the top of the shell-side as a dispersed two-phase stream which evaporates while streaming towards the bottom of the CWHE. The natural gas liquification is driven by the complex thermodynamic interaction across the tube bundle with the multiphase flow at the shell-side of the CWHE. The gas-liquid flow characteristics determine local heat transfer and affect the efficiency and functionality of the entire apparatus.

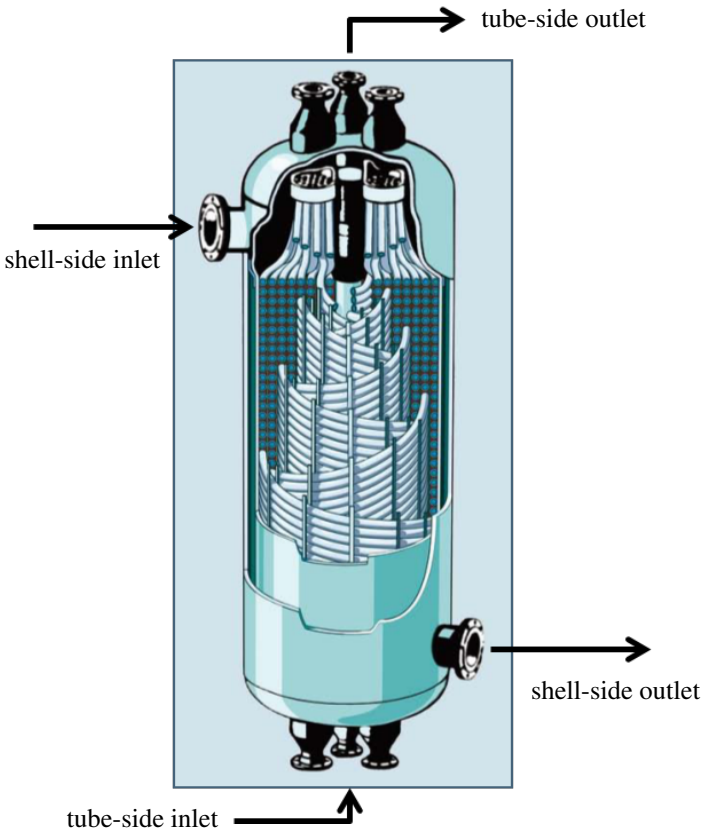

Figure 1: Exemplary sketch of a coil-wound heat exchanger.

In general, one-dimensional correlations are applied to represent fluid and thermodynamic processes in order to design CWHE apparatuses (Wang *et al.*, 2015). Merely axial variations of thermohydraulic parameters are captured by this approach while radial parameter variations, specifically fluiddynamic inhomogeneities, are neglected. In order to incorporate these potentially influential phenomena a two-dimensional CFD model has been developed. The following sections explicate this approach, specifically the gas-liquid flow representation as well as the effect of radial varying geometry parameters at the shell-side. Remaining model constants are specified by parameterization and CFD model results are presented.

CFD MODEL DESCRIPTION

A numerically efficient representation of the CWHE is realized by the consideration of a two-dimensional cross-section of the cylindrical form (see Fig. 2). While assuming rotational symmetry of the apparatus, radial variations of thermohydraulic parameters are represented by this modeling setup. The individual fluid dynamic regions on the shell-side and the tube-side of the CWHE are reflected by separate simulation domains, where multiple tube sections are represented individually. To model the heat transfer between the shell- and the tube-side the independent flow regions are thermodynamically coupled by respective source terms and the hydraulic effect of the tube bundle is represented as a porous medium with corresponding fluid dynamic characteristics. This setup enables a coherent decomposition of the numerical meshes of the individual domains to allow for an efficient computation on multiple processors.

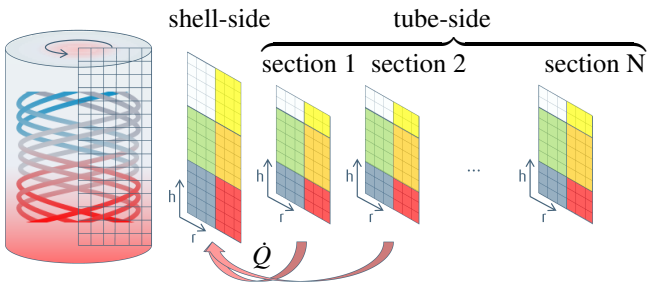

Figure 2: Two-dimensional representation of the CWHE with a shell-side domain and multiple tube sections (Göll *et al.*, 2013).

The fluid dynamics at both the tube- as well as the shell-side of the CWHE are modeled by an Euler-Euler approach (e.g., (Drew and Passman, 1999; Ishii and Hibiki, 2010)) since two-phase flows may occur at any flow region. The respective transport equations for momentum read

$$\frac{\partial}{\partial t}\alpha_i\rho_i\vec{u}_i+\nabla\cdot\alpha_i\rho_i\vec{u}_i\vec{u}_i = -\alpha_i\nabla p_i+\nabla\cdot\alpha_i\underline{\tau_i}+\alpha_i\rho_i\vec{g}+\vec{f}_{rad,i}+\vec{f}_{h,i} \quad (1)$$

where α_i, ρ_i, $\vec{u}_i$ and τ_i denote the volume fraction, density, velocity and shear stress tensor of phase i. The fluid dynamic interaction between gas and liquid as well as the flow resistance in the porous media are modeled by the phase specific body forces in axial direction $f_{h,i}$ and radial direction $f_{rad,i}$.

The Euler-Euler CFD solver *twoPhaseEulerFoam* of the program package OpenFOAM represents the basis for the model implementation which is interfaced to submodels for the evaluation of local void fractions and fluid parameters, pressure drop in the porous media and transferred heat between flow regions (see Fig. 3). In contrast to classical Euler-Euler models, local phase fractions are computed from the local composition of chemical species and thermodynamic conditions which requires the inclusion of transport equations of the comprised species instead of a respective formulation for local void fraction. Local thermodynamic equilibrium is assumed to determine relevant fluid properties (i.e. viscosity, density, thermal

conductivity and surface tension) and phase composition in each numerical cell based on local species concentrations and thermodynamic relations (Jakobsen, 2008). Local thermodynamic conditions are computed from the energy transport equation which includes source terms for the heat transfer across the simulation domains.

As depicted in Fig. 3 the evaluation of fluid parameters at vapor/liquid-equilibrium in each numerical cell is realized by coupling the CFD solver to Linde's inhouse software. This program is used for cell-wise conduction of flash calculations (pH-flash) in order to evaluate local phase fractions and fluid properties. Energy transport equation source terms which represent heat transfer effects are based on one-dimensional correlations used for CWHE design at Linde which are determined by flow parameters and single- or two-phase flow conditions. At the shell-side as well as at the tube-side, the flow resistance due to the tube bundle is integrated in the CFD model by a porous zone. The corresponding pressure drop properties are evaluated from CWHE design correlations analogous to the heat transfer calculations. For additional information on the CFD model framework the reader is referred to previous publications (Acher *et al.*, 2016).

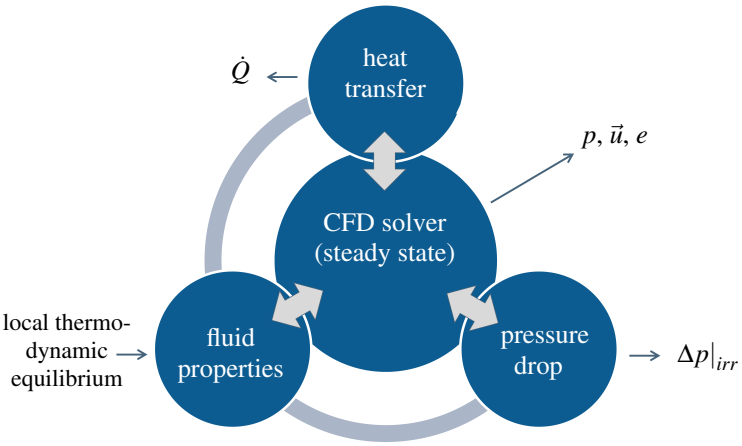

Figure 3: Depiction of numerical model components and their interaction.

As mentioned above, potential radial variations of fluid dynamic parameters might impact the heat transfer performance of the CWHE. These non-uniformities can originate from two-phase flow effects on the shell-side of the apparatus. The consideration of these phenomena necessitates the incorporation of submodels for an enhanced depiction of gas-liquid flow conditions.

Two-phase flow model development

The shell-side of the CWHE features a gas-liquid flow which is applied as a dispersed stream above the tube bundle and evaporates on its way to the bottom of the apparatus. The related thermohydraulic effects are commonly depicted by empirical correlations which resort to pseudo-homogenous parameters describing the multiphase flow. In contrast, in an Euler-Euler context the prevalent retaining and interfacial forces have to be modeled individually to yield phase-specific velocity fields (see Fig. 4).

In order to ensure consistency with the pseudo-homogeneous concept for a radially uniform flow field, the two-phase pressure drop characteristics along the bundle are

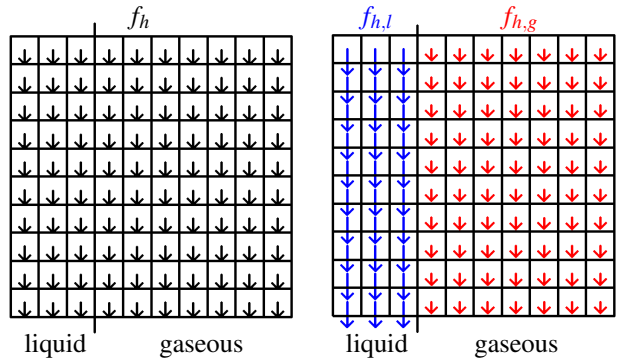

Figure 4: Schematic depiction of the volume force acting on fluid elements in a numerical cell (Knaup, 2015). Left: pseudo-homogenous flow resistance. Right: phase-specific flow resistance.

retained as specified by the one-dimensional model and the homogeneous force field f_h is divided into phase-specific contributions $f_{h,i}$:

$$f_{h,i} = C_i f_h = \frac{f_{ax,i}}{f_{ax,j} + f_{ax,i}} f_h \tag{2}$$

where the weighting coefficient C_i is a function of the axial forces acting on the gas phase $f_{ax,g}$ and the liquid phase $f_{ax,l}$ inside the tube bundle.

The axial retaining and interfacial forces for the individual phases $f_{ax,g}$ and $f_{ax,l}$ are further subdivided according to the bilateral interaction between gas, liquid and tube bundle. To do so, a basic perception of the gas-liquid flow pattern in the tube bundle is required. Figure 5 depicts the assumed liquid flow structures on the shell-side of the tube bundle which are comprised of vertical films enclosing the coiled tubes and dispersed droplets between tube layers.

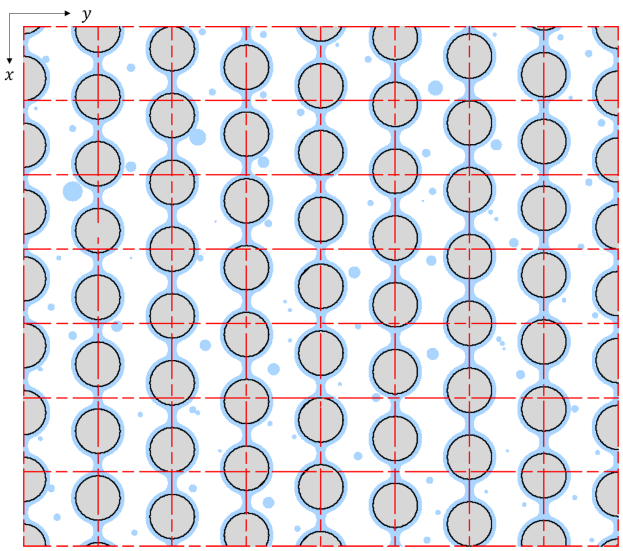

Figure 5: Sketch of the presumed gas-liquid flow conditions at the shell-side of the CWHE bundle

Due to their fundamentally different characteristics with regard to gas-liquid interaction the liquid film and droplets are modeled independently. Hence, the axial phase-specific forces at the shell-side are formulated as

$$f_{ax,g} = f_{gs} + f_{gl,d} + f_{gl,f}, \tag{3}$$

$$f_{ax,l} = f_{ls} - f_{gl,d} - f_{gl,f}. \quad (4)$$

Table 1 gives a description on each of the phase-specific interfacial forces and states the modeling approach selected for their evaluation. As the gas-liquid interaction $f_{gl,d}$ is a function of the volume fraction of liquid droplets and drop sizes these parameters are derived from model correlations based on local fluid dynamic equilibrium considerations (Sirignano, 2010; Ishii and Mishima, 1989). Consistent to experimental observations, it is assumed that liquid velocities are dominated by the film around the tubes as the volumetric contribution of droplets is considered subordinate. This conception arguably justifies the adoption of simple approaches for the evaluation of droplet sizes and local volume ratios of droplet to film. Yet, this assumption is further validated by detailed 3D CFD simulations presented below.

Analogous to the representation of phase-specific axial forces the numerical model includes a formulation for radial volume forces $f_{rad,i}$ in the Euler-Euler momentum equations Eqn. 1. Two prevalent mechanisms which induce radially acting volume forces were identified based on experimental findings, operational data analysis and detailed 3D CFD simulation of single- and multiphase flows. Table 2 gives a brief description of both the lift and centrifugal force. A more detailed explication with a focus on the origin of both effects with regard to the apparatus at hand is part of the following subsections.

The phase-specific cumulated effect of radial fluid dynamic processes is incorporated as

$$f_{rad,l} = f_{lift,l} + f_{cent,l}, \quad (5)$$

$$f_{rad,g} = -f_{lift,g} + f_{cent,g}. \quad (6)$$

The formulations for both radially acting forces $f_{lift,i}$ and $f_{cent,i}$ feature a model constant which has to be adjusted to experimental findings and is further explicated in the last section of this work.

The subdivision of retaining and interfacial forces $f_{h,i}$, explicated above, is a prerequisite to the evaluation of radial fluid dynamic processes as the respective models for $f_{lift,i}$ and $f_{cent,i}$ depend on individual phase velocities u_i. Locally determined phase-specific velocities which are inaccessible to common one-dimensional CWHE design correlations are required to investigate radial inhomogeneity of the two-phase flow on the shell-side of the apparatus. Radial parameter variations in the CWHE can be ascribed to radial inhomogeneity of the two-phase flow on the shell-side which impacts the efficiency of heat transfer processes.

Incorporation of the centrifugal force

The helical motion of gas in between the coiled tube rows as sketched in Fig. 6 effects a centrifugal force which is directed radially outward independent of the tube layer coiling direction. The gaseous flow pattern was confirmed by three-dimensional numerical simulations of single-phase flow through the resolved bundle geometry. It is assumed that liquid droplets follow this spiral motion (analogous to the flow in a cyclone used as a separator) and consequently are subject to the centrifugal force in radial direction.

Incorporation of the lift force

The lift force effect is initiated from radial variation of the axial gas flow velocity due to the geometrical inhomogeneity

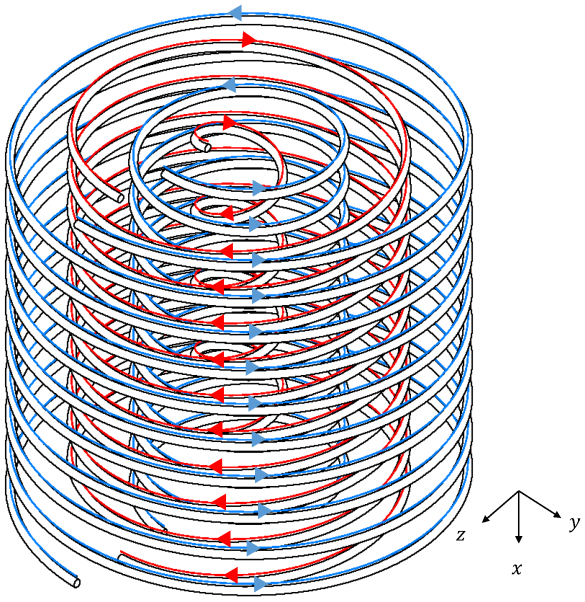

Figure 6: Delineation of the helical gas flow alternating in orientation for each tube layer. The arrows indicate the direction of the gas motion.

of the tube bundle. To illustrate this connection, a section of a CWHE tube bundle geometry for an experimental setup is depicted in Fig. 7. It shows several layers of coil-wound tubes in between the central pipe (i.e. the mandrel) and the outer shroud of the apparatus. A constant distance between tube rows and layers is maintained by tube spacers which are depicted in Fig. 7 in an abstracted manner by vertical beams. At different radii the spacers block varying portions of the free space between two layers of wound tubes. This results in a radial dependency of shell-side flow resistance which is to be adopted in the numerical modeling.

The non-uniform blocking of the free area between tube layers is represented in the CFD model via radially variant values of porosity defined as the ratio of actual void area to void area without any spacers:

$$\varepsilon = \frac{A_{void} - A_{spacer}}{A_{void}} \quad (7)$$

Using this values of porosity a representative gas velocity for a heat exchanger without spacers can be derived from the local gas velocity:

$$u_{g,\infty} = \left(\frac{1}{\varepsilon}\right)^{a} \cdot u_g \quad (8)$$

This velocity is the input for the calculation of the homogenous flow resistance f_h in equation 2 and leads to a radially varying flow resistance generating a velocity profile which can be adjusted by the coefficient a in equation 8. The parameter a is deduced from single phase 3D CFD simulations of the shell side flow through a representative section with detailed resolution of the tube bundle geometry as explained in the following section.

Submodel validation and parametrization

The aforementioned setup for the calculation of the gas-liquid flow through a coil wound heat exchanger requires many different sub-models, whose accuracy is crucial for

Table 1: Considered phase-specific axial forces on the two-phase flow at the shell-side of the CWHE bundle

	Description	Evaluation method
Gas-solid interaction f_{gs}	Retaining force on the gas flow by the partial blocking of the flow cross-section	Evaluation from single phase pressure drop correlation (Steinbauer and Hecht, 1996)
Liquid-solid interaction f_{ls}	Liquid film flow resistance due to tube wall friction	Adaption of the Nusselt water skin theory to flow across tubes (Rogers, 1981)
Gas-liquid droplet interaction $f_{gl,d}$	Drag force on droplets induced by the gaseous flow	Calculation from conventional drag force model (Schiller and Naumann, 1935)
Gas-liquid film interaction $f_{gl,f}$	Shear forces at the fluidic interface between gas and liquid film	Effect is considered as subordinate and therefore neglected

Table 2: Considered radial forces on the two-phase flow at the shell-side of the CWHE bundle

	Description	Evaluation method
Droplet lift force $f_{lift,i}$	Radial force on the droplet due to inhomogeneous gas flow through the porosity	Determination from common lift force approach with an adapted coefficient (Ishii and Hibiki, 2010)
Centrifugal force $f_{cent,i}$	Centrifugal effect on liquid droplets due to rotational motion of the gas	Definition of the centrifugal force on the droplet with a model factor

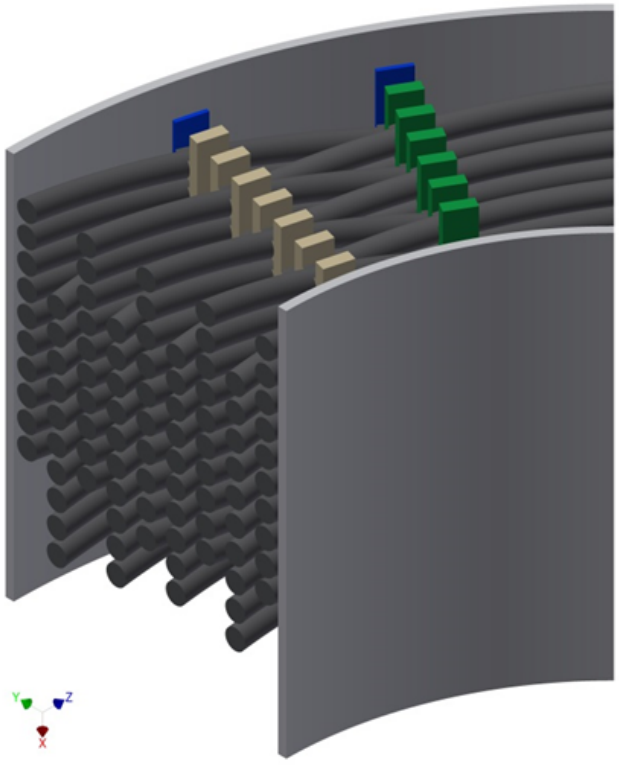

Figure 7: CAD model of a section of an experimental CWHE tube bundle with highlighted tube spacers. (Kiewat, 2015)

the correct prediction of the heat transfer inside the bundle. These models were derived under several assumptions and so have to be validated and parametrized with numerical and experimental data.

For the numerical investigation a CFD simulation resolving the gas-liquid and liquid-solid interface and most of the turbulence spectrum is required. In this case, the Volume-of-Fluid (VOF) method for the two-phase flow is coupled with an LES approach for the description of turbulence. With this approach the phase interaction and the effects of turbulence are derived directly from the Navier-Stokes-Equations instead of physical models.

The VOF approach is accompanied by a high computational effort to resolve most of the relevant length scales. In this case the smallest cell size was chosen to have a dimension of about 10 micrometers to resolve the vast majority of expected droplets. The total number of cells is decreased by limiting the simulation domain to a representative cutout of a coil wound heat exchanger using periodic boundary conditions as depicted in Figure 8 for one tube layer.

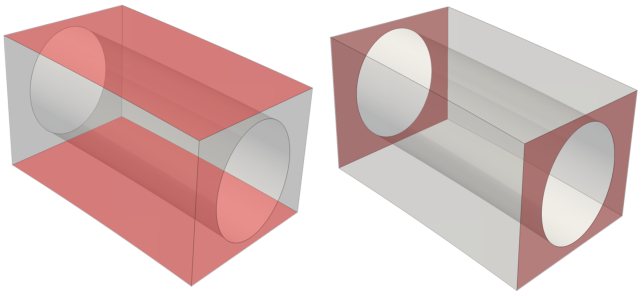

Figure 8: Schematic depiction of the periodicities in one layer of a coil wound heat exchanger (Bassfeld, 2017). Left: periodicity in axial direction; Right: periodicity in azimuthal direction.

To account for the interaction within the coil three layers were considered in the simulation setup. To this end, the non-overlapping boundaries resulting from the different orientated slope in the layers were associated with periodic boundary conditions as can be seen in Figure 9. As only fluiddynamical aspects were examined here, the flow was

regarded as incompressible without heat transfer from the tube-side or vaporization of the shell-side flow.

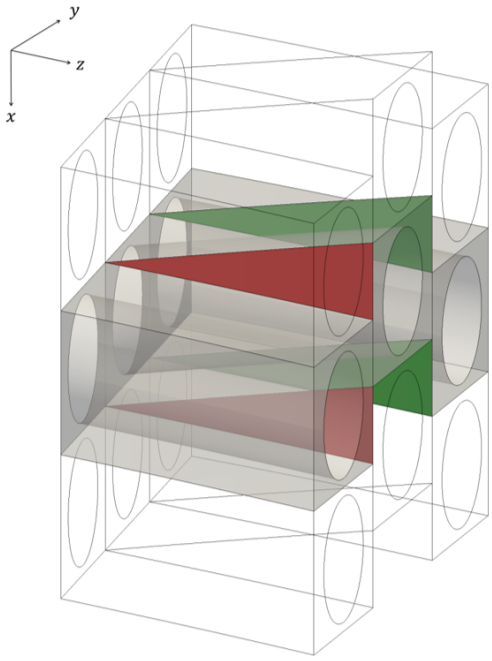

Figure 9: Schematic depiction of the periodicities in radial direction. (Bassfeld, 2017). Same colour indicates periodic connection. For better comprehension also one section above and below is depicted in transparent.

Figure 10 shows an instantaneous depiction of the liquid phase distribution which is color-coded by the local velocity. This confirms the current perception of gas-liquid pattern in the coil as shown in Figure 5. Especially the droplets' volume fraction of the whole liquid could be determined to about 0.05, justifying the rather simple approach for the droplet interaction in the previous section.

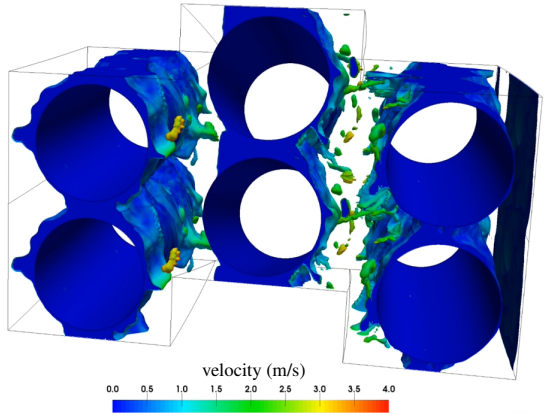

Figure 10: Isometric view of the liquid flow inside the tube bundle. (Bassfeld, 2017).

Most of the liquid is present as a falling film while the reminder forms droplets which are generated by liquid separation from film waves. These droplets are transported away from the tube layer and cause the radial migration of liquid. The accumulated effect is captured by the radial fluid interaction submodels in the Euler-Euler context in an abstracted manner.
The helical gas motion as sketched in Figure 6 is confirmed by the averaged velocity field resulting from the VOF simulation. Figure 11 depicts the respective azimuthal component of the time-averaged gas flow indicating the swirl flow pattern.

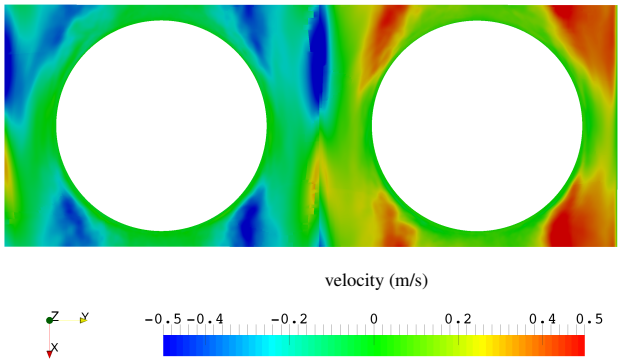

Figure 11: Plot of the azimuthal velocity component of the gas flow. (Bassfeld, 2017).

To determine the coefficients for the radial profile of the axial gas velocity a single phase RANS simulation was performed. The resulting profile is depicted in Figure 12. By adapting the coefficient a in equation 8 to a value of 2.5 this velocity profile could be reproduced in the Euler-Euler model.

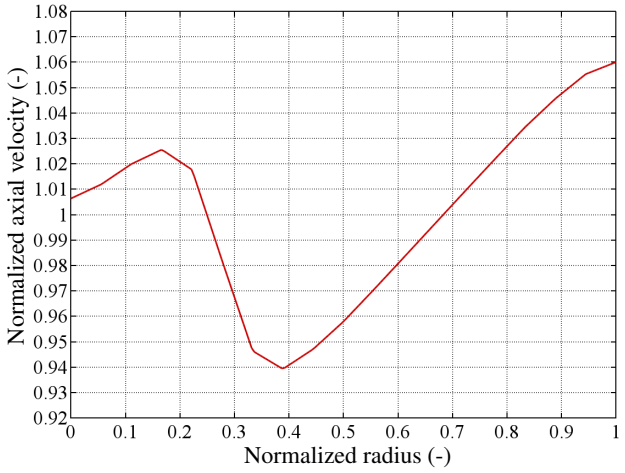

Figure 12: Plot of the axial velocity component of the gas flow over the radius. Local velocity values are normalized by average axial velocity.

To supplement the numerical data also an experimental campaign was launched using a pilot scale CWHE (see (Walter *et al.*, 2014) for details). It completes the validation data set for the measurement of the radial liquid distribution for many different flow conditions with and without heat transfer. These results were used for a parametrization study in order to specify model constants in the definition of the radial forces $f_{lift,i}$ and $f_{cent,i}$

MODEL RESULTS

The final model setup was then used to simulate various experimental cases and the measured radial variation of the liquid distribution below the tube bundle was used to validate the CFD model setup.
The simulation results of the numerical model with a fixed parameter set show good accordance with the experimental findings for the entire spectrum of investigated fluid dynamic

parameters. As an example, a comparison of numerical and experimental results for two cases with strongly varying vapor quality is shown in Figures 13 and 14.

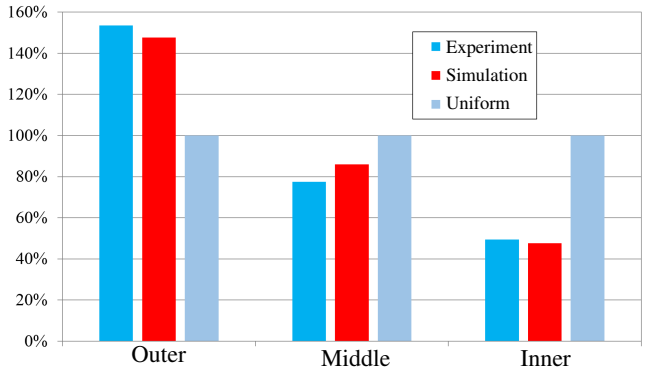

Figure 13: Liquid flow distribution at the bottom of the tube bundle for an experimental case with high gas throughput.

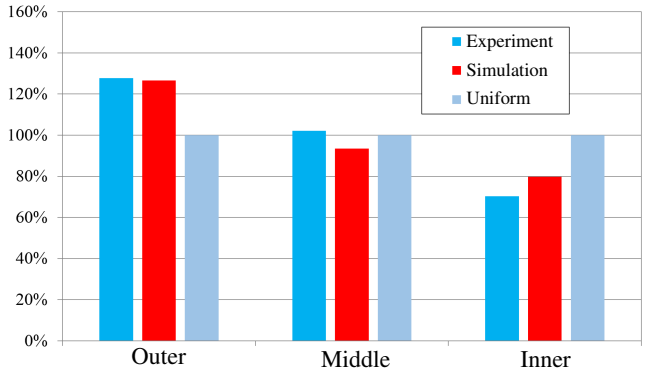

Figure 14: Liquid flow distribution at the bottom of the tube bundle for an experimental case with low gas throughput.

CONCLUSION

A two-dimensional CFD model was introduced in the present work to represent the thermo- and fluid-dynamic processes in a coil-wound heat exchanger. Specifically the representation of the gas-liquid hydrodynamics is explicated with a focus on the incorporation of retaining and interfacial forces.

The model framework represents a modified Euler-Euler approach adopting the concept of local thermodynamic equilibrium to determine volume fractions and phase properties. The local heat transfer across the exchanger fluid regions is represented by one-dimensional model formulations which are commonly used for coil-wound heat exchanger design. These thermohydraulic correlations also determine the characteristics of the porous media model to consider the impact of the tube bundle on the fluid dynamics through and within the tube bundle.

The representation of individual retaining and interfacial forces at the shell-side of the tube bundle enables the computation of phase-specific velocities. In association with the consideration of radial geometry variations the differences in the phase velocities effect a radial motion of the liquid. This effect is superimposed by a centrifugal effect which is induced by the helical motion of the gaseous phase phase following the coiled tubes. Both fluid-dynamic processes are represented in the numerical model by the incorporation of corresponding source terms in the momentum equations.

Detailed 3D CFD simulation and experimental investigations have been conducted in order to validate specifics of phase interaction models. The Volume-of-fluid simulations indicated local liquid flow conditions, specifically with regard to droplet sizes, quality and behavior. Additionally these investigations confirmed observations regarding helical gas flow for a multiphase system. The experimental results were used to obtain the coefficients for the radial forces.

A comparison with experimental findings showed that the present two-dimensional CFD model was able to simulate the inhomogeneity of cross-sectional liquid distribution with agreement to measured values over a broad range of flow conditions.

REFERENCES

ACHER, T., KNAUP, M., GÖLL, S., ZANDER, H.J., LENZ, S. and KERBER, C. (2016). "A two-dimensional CFD model for gas-liquid flows in a coil-wound heat exchanger". *Proceedings of the 9th International Conference on Multiphase Flow*.

BASSFELD, J. (2017). *Untersuchung der Hydrodynamik in gewickelten Wärmetauschern*. Master's thesis, Technische Hochschule Nürnberg Georg Simon Ohm.

DREW, D. and PASSMAN, S. (1999). *Theory of multicomponent fluids*. Springer.

GÖLL, S., ZANDER, H.J., LENZ, S. and KERBER, C. (2013). "Entwicklung eines 2D-CFD-Modells zur Berechnung der Wärmeübertragung in spiralgewickelten Wärmeaustauschern". *Jahrestreffen der ProcessNet-Fachgruppen CFD, Mischvorgänge und Rheologie Würzburg*.

ISHII, M. and HIBIKI, T. (2010). *Thermo-fluid dynamics of two-phase flow*. Springer.

ISHII, M. and MISHIMA, K. (1989). "Droplet entrainment correlation in annular two-phase flow". *Int. J. Heat Mass Transf.*, **32**, 1835–1846.

JAKOBSEN, H. (2008). *Chemical reactor modeling: multiphase reactive flows*. Springer.

KIEWAT, M. (2015). *CFD SIMULATION OF COIL WOUND HEAT EXCHANGERS*. Master's thesis, Friedrich-Alexander-Universität Erlangen-Nürnberg.

KNAUP, M. (2015). *Modellierung und numerische Simulation der Zweiphasenströmung in einem spiralgewickelten Wärmetauscher*. Master's thesis, Technische Universität München.

PACIO, J.C. and DORAO, C.A. (2011). "A review on heat exchanger thermal hydraulic models for cryogenic applications". *Cryogenics*, **51**, 366–379.

ROGERS, J.T. (1981). "Laminar Falling Film Flow and Heat Transfer Characteristics on Horizontal Tubes". *Can. J. Chem. Eng.*, **59**, 213–222.

SCHILLER, L. and NAUMANN, K. (1935). "Über die grundlegenden Berechnungen bei der Schwerkraftaufbereitung". *Zeitschrift des Vereins der deutschen Ingenieure*, **77**, 316–320.

SIRIGNANO, W. (2010). *Fluid Dynamics and Transport of Droplets and Sprays*. Cambridge University Press.

STEINBAUER, M. and HECHT, T. (1996). "Optimised Calculation of Helical-Coiled Heat Exchangers in LNG Plants". *Eurogas 96 Conference*.

WALTER, T., KERBER, C., BRAUN, K., RICHARDT, C. and STEINBAUER, M. (2014). "Coil wound heat exchangers for LNG - investigation of transport phenomena within the bundle". *Proceedings of the 3rd Trondheim Gas Technology Conference*.

WANG, T., DING, G., DUAN, Z., REN, T., CHEN, J. and PU, H. (2015). "A distributed-parameter model for LNG spiral wound heat exchanger based on graph theory". *Applied Thermal Engineering*, **81**, 102 – 113.